




Recruitment of CTCF to an *Fto* enhancer is responsible for transgenerational inheritance of BPA-induced obesity

Yoon Hee Jung^{a,1}, Hsiao-Lin V. Wang^a, Daniel Ruiz^a, Brianna J. Bixler^a, Hannah Linsenbaum^a, Jian-Feng Xiang^a, Samantha Forestier^a, Andrew M. Shafik^a, Peng Jin^a , and Victor G. Corces^{a,2} 

Contributed by Victor G. Corces; received September 1, 2022; accepted November 10, 2022; reviewed by Juan Ausio, Qi Chen, and Wei Xie

The mechanisms by which environmentally-induced epiphenotypes are transmitted transgenerationally in mammals are poorly understood. Here we show that exposure of pregnant mouse females to bisphenol A (BPA) results in obesity in the F2 progeny due to increased food intake. This epiphenotype can be transmitted up to the F6 generation. Analysis of chromatin accessibility in sperm of the F1–F6 generations reveals alterations at sites containing binding motifs for CCCTC-binding factor (CTCF) at two cis-regulatory elements (CREs) of the *Fto* gene that correlate with transmission of obesity. These CREs show increased interactions in sperm of obese mice with the *Irx3* and *Irx5* genes, which are involved in the differentiation of appetite-controlling neurons. Deletion of the CTCF site in *Fto* results in mice that have normal food intake and fail to become obese when ancestrally exposed to BPA. The results suggest that epigenetic alterations of *Fto* can lead to the same phenotypes as genetic variants.

chromatin | transcription | sperm | oocyte | fertilization

Evidence suggestive of inter- and transgenerational inheritance of epiphenotypes in mammals has been reported extensively (1–3). For example, exposure of laboratory animals or humans to endocrine-disrupting compounds leads to increased reproductive dysfunction, cancer, obesity, diabetes, and behavioral disorders (4). However, we still lack an understanding of the molecular processes by which epigenetic alterations induced by the environment are transmitted between the exposed and subsequent generations in mammals. This is in part due to the peculiar state of the nucleus in the mature gametes, which is highly condensed in sperm and arrested in metaphase II in mature oocytes. In addition, the epigenetic content of the mammalian germline in the form of DNA methylation is reprogrammed at least twice in each life cycle, once during the differentiation of the primordial germ cells (PGCs) and a second time after fertilization during pre-implantation development of the embryo (5). This erasure of epigenetic information complicates the mechanistic interpretation of well-documented observations. Mechanisms involving small RNAs have been successful in explaining transgenerational phenomena in *C. elegans*, where these RNAs can be amplified by RNA-dependent RNA polymerases in each generation (6). The contribution of small RNAs present in the gametes to the transmission of epiphenotypes between generations has also been explored in mammals, perhaps in part due to the apparent lack of reprogramming-resistant epigenetic information that can serve as memory of ancestral environmental influences. For example, transfer RNA (tRNA) fragments made in the epididymis and transported to sperm have been implicated in intergenerational transmission of metabolic effects caused by paternal protein restriction or high fat diet (7, 8). micro RNAs (miRNAs) present in sperm and transferred to the zygote may also cause changes in gene expression affecting the differentiation of adult tissues and have been suggested to be responsible for the transmission of behavioral and metabolic changes caused by early life traumatic stress (7–10). However, there is no current evidence supporting a role for small RNAs in the transmission of environmentally induced phenotypes through multiple generations in mammals.

Transcription factors (TFs) sit at the top of the cascade of events that lead to gene expression and are causal to many of the chromatin features normally considered to carry epigenetic information. It is thus possible that TF occupancy cooperates with DNA methylation or covalent histone modifications to retain epigenetic information through reprogramming events in the germline or the early embryo. This has been shown to be the case for TFs that protect their binding sites from re-methylation both during germline development and in the blastocyst (11). A variation on this idea is represented by the interplay between placeholder nucleosomes containing the histone variant H2A.Z and DNA methylation, which has been shown to mediate transmission of information between the gametes and embryos in zebrafish (12). Therefore, memory of ancestral epigenetic alterations caused by environmental changes may be encoded by a combination of reprogramming-resistant

Significance

Exposure of pregnant female mice to bisphenol A (BPA) results in obesity in the F2 progeny, which can be transmitted in the absence of additional exposure up to the F6 generation. Obesity results from increased food consumption and its transmission correlates with the presence of a chromatin accessible site in a cis-regulatory element (CRE) present in an intron of the *Fto* gene, which becomes demethylated after BPA exposure. This CRE interacts with the *Irx3* and *Irx5* genes, which are involved in the differentiation of appetite-controlling neurons in the hypothalamus. Mice carrying a deletion of the CTCF site fail to become obese after exposure to BPA, suggesting that epigenetic changes in a CTCF site are responsible for transgenerational inheritance of obesity.

Author contributions: Y.H.J., H.-L.V.W., P.J., and V.G.C. designed research; Y.H.J., H.-L.V.W., D.R., B.J.B., H.L., J.-F.X., S.F., and A.M.S. performed research; Y.H.J., H.-L.V.W., D.R., B.J.B., and V.G.C. analyzed data; and Y.H.J., H.-L.V.W., D.R., and V.G.C. wrote the paper.

Reviewers: J.A., University of Victoria; Q.C., University of California; and W.X., Tsinghua University.

The authors declare no competing interest.

Copyright © 2022 the Author(s). Published by PNAS. This article is distributed under Creative Commons Attribution-NonCommercial-NoDerivatives License 4.0 (CC BY-NC-ND).

¹Present address: Department of Physiology, Ajou University School of Medicine, Suwon, 16499, Republic of Korea.

²To whom correspondence may be addressed. Email: vgc@corces@gmail.com.

This article contains supporting information online at <https://www.pnas.org/lookup/suppl/doi:10.1073/pnas.2214988119/-/DCSupplemental>.

Published December 5, 2022.

molecular events during critical periods of the life cycle, such as germline differentiation and pre-epiblast development, together with more classical epigenetic information at other stages of cell differentiation.

Bisphenol A (BPA) is used in the manufacturing of plastics, and it is ubiquitously present in the environment (13). BPA has estrogenic activity (14), and exposure to this compound has complex health effects that include obesity, skeletal system dysfunction, behavioral problems, and effects on reproductive organs, which can be transmitted up to the F3 generation (15–18). Here we use BPA-induced obesity as a paradigm to study the mechanisms by which epiphenotypes can be transmitted through the mammalian germline. We find that obesity elicited by exposure of pregnant P0 females to BPA is the result of increased food consumption, can be transmitted through the male and female germlines, and down to the F6 generation. Using the assay for transposase-accessible chromatin by sequencing (ATAC-seq) to identify accessible sites in the genome of the gametes bound by TFs and correlating this information with transmission of obesity, we identify several sites containing motifs for CTCF, FOXA1, estrogen receptor alpha (ESR1), and androgen receptor (AR) present in two CREs of the *Fto* gene in obese but not control mice. These cis-regulatory elements (CREs) show increased interactions with the *Irx3* and *Irx5* genes in sperm of BPA-exposed versus control mice. Mouse strains carrying a deletion of a 343 bp region containing the CTCF-binding motif in one of the *Fto* CREs fail to transmit the obesity epiphenotype to subsequent generations when ancestrally exposed to BPA. Since regulatory sequences present in the *Fto* gene have been previously shown to regulate the expression of *Irx3* and *Irx5*, we suggest that BPA-induced obesity may affect expression of these two genes and alter the differentiation of appetite-controlling neurons in the hypothalamus.

Results

Exposure of Pregnant Mouse Females to BPA Causes Obesity that Can Be Transmitted Transgenerationally. To gain insights into the mechanisms by which epiphenotypes elicited by environmental exposures can be transmitted transgenerationally, we examined the effect of the endocrine-disrupting chemical BPA. Previous work has shown that exposure of pregnant rats and mice to a variety of endocrine disruptors during the window of time when the germline of the embryo is demethylated leads to various health effects in the progeny, including testicular and breast cancer, behavioral defects, and obesity (17, 19–21). Following this established work, we exposed two pregnant female mice (P0) via daily intraperitoneal injection of BPA (50 mg/kg body weight/day) during days E7.5 through E13.5 of fetal development (15). This amount of BPA is much higher than what most humans are exposed to (22), and experiments described below analyze the effect of lower concentrations. As a control, two pregnant females were injected with vehicle only (see *Materials and Methods* for details). In the rest of the manuscript, we will refer to the progeny of BPA-exposed P0 females as BPA-Fi, where *i* is the generation number, and the progeny of vehicle-exposed females as control-Fi (CTL-Fi), although the exposure took place only in the P0 generation. The BPA-F1 male progeny shows no statistically significant differences in body weight when compared to CTL-F1 or to male siblings of the P0 females (*SI Appendix, Fig. S1A*). One CTL-F1 male and one CTL-F1 female were then crossed. Similarly, one BPA-F1 male was crossed to one BPA-F1 female from a parallel exposure experiment (*SI Appendix, Fig. S1B*). Males and females for this and other crosses described in the manuscript were selected to have a weight similar to the

median for their litters. BPA-F2 males from this cross displayed a statistically significant increase in body weight with respect to CTL-F2 and P0 males (*SI Appendix, Fig. S1A*). However, CTL-F2 males have statistically the same weight as CTL-F1 and P0 males, suggesting that exposure to the sesame oil vehicle has no effect on body weight, as has been previously shown (21). Therefore, unless specifically indicated, in the rest of the manuscript we will use the unexposed siblings of the P0-exposed females as controls for changes in body weight of mice ancestrally exposed to BPA.

Crosses between BPA-Fi males and BPA-Fi females were continued as described in *SI Appendix, Fig. S1B*. The increased body weight was also observed in the BPA-F3 through BPA-F6 generations, but BPA-F7 animals had a weight similar to that of controls (*Fig. 1A*). The same experiment was performed a second time and weights were monitored up to the F7 generation. In four additional experiments, weights were monitored for the F1–F4 generations but crosses were not continued past F4. The results in *Fig. 1A* represent the male mice from these six experiments. Results from an additional experiment encompassing the F1–F3 generations are shown below *Fig. 5 A and B*. To compare changes in body weight in different generations, we took the mean weight of control males at week 10 and we defined obese animals as those whose weight at this age is one SD above the mean control weight. Only 8% of males are overweight in the BPA-F1 generation by this criterion, which is similar to control (*Fig. 1B*). The fraction of overweight males increases to 60% in BPA-F2, peaks at 97% in BPA-F4, and starts decreasing through BPA-F5–6. Approximately 60% of F6 males are obese and 40% have normal weight; we will refer to these F6 mice with normal weight as “lean.” All BPA-F7 males display weights similar to those of control males (*Fig. 1B*). Body weight of BPA-Fi mice of any generation is the same as that of controls at 3 wk of age, but differences become statistically significant by weeks 5 to 6 and remain for the rest of adult life (*Fig. 1C*). These differences are more pronounced in males than females (*Fig. 1C* and *SI Appendix, Fig. S1C*). Crosses between overweight or between lean BPA-F6 animals produce progeny with weights statistically indistinguishable from those of controls (*SI Appendix, Fig. S1D*), suggesting that the germline of F6 animals has lost the information responsible for the inheritance of obesity independent of the weight of the animals.

BPA-Fi mice show a large accumulation of visceral white adipose tissue (WAT) compared to controls (*Fig. 1D, Top*) and increase in the size of adipocytes (*Fig. 1D, Bottom*). Whereas the visceral WAT represents 1.32% of total body weight in control male animals, this value increases to 2.45% in BPA-F4 males ancestrally exposed to BPA (*Fig. 1E*). The serum levels of leptin in mice ancestrally exposed to BPA increase with age following the increase of body weight. At 3 wk of age, leptin levels are the same in BPA-exposed and control but differences between the two groups increase at 6 wk and 12 wk (*Fig. 1F*). We also examined the presence of stem cell antigen-1 (SCA-1) positive cells by performing immunofluorescence microscopy with antibodies to SCA-1, which label adipocyte progenitor cells as well as hematopoietic precursors (*SI Appendix, Fig. S1E*). Results show that 69% of the cells in fat tissue from BPA-F4 males correspond to SCA-1 positive cells compared to 22% in the fat tissue of control animals (*SI Appendix, Fig. S1F*).

It has been estimated that humans are exposed to an average of 50 µg/kg body weight of BPA (23), resulting in concentrations of this compound in serum in the ng per mL range (24). Since the amount of BPA to which mouse pregnant females are exposed in our experiments is much higher than that to which the average human is thought to be exposed, we injected pregnant females with decreasing concentrations of BPA and examined the effect on body

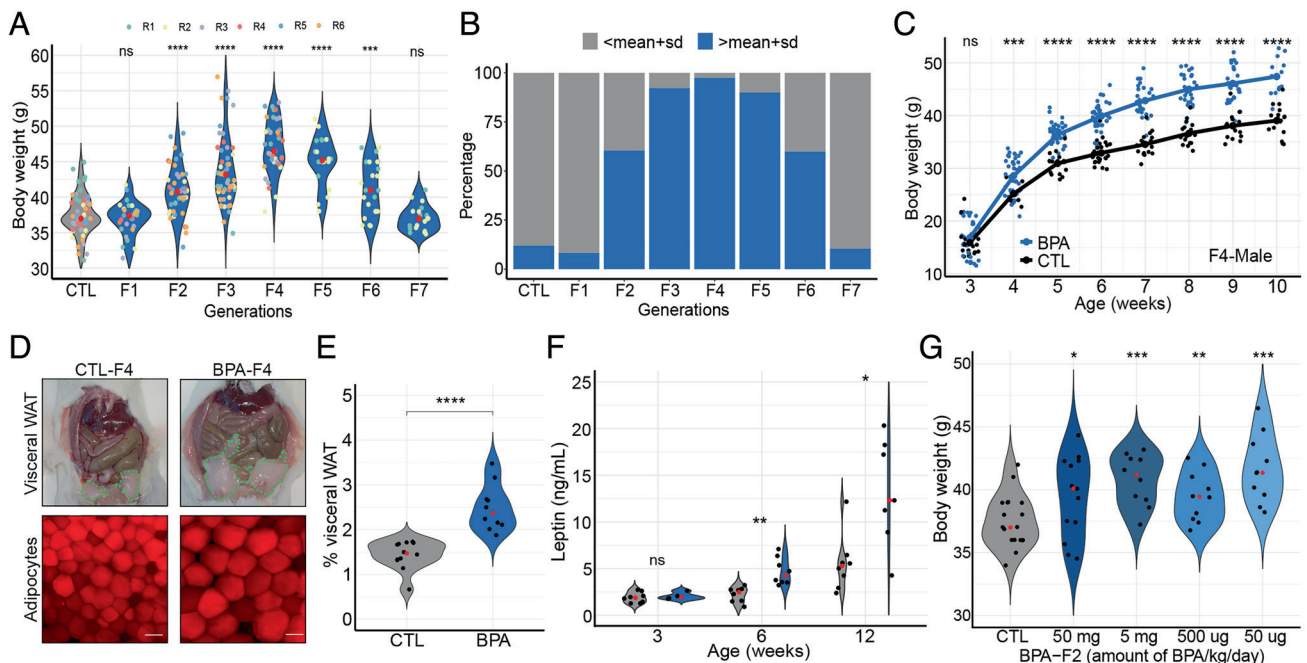


Fig. 1. Analysis of BPA-induced obesity. (A) Changes in body weight between control and different generations of the male progeny of BPA-exposed P0 pregnant female mice at 10 wk of age. Results represent a combination of six different independent experiments in which 12 different females were exposed to BPA and crossed following the outline shown in *SI Appendix, Fig. S1B*. Four of these experiments were stopped at the F4 generation whereas two were continued up to the F7 generation. The number of mice analyzed were CTL $n = 57$, F1 $n = 28$, F2 $n = 43$, F3 $n = 55$, F4 $n = 41$, F5 $n = 20$, F6 $n = 25$, and F7 $n = 19$. (B) Percentage of obese mice in the F1–F7 generation progeny of BPA-exposed P0 pregnant females. Obese is arbitrarily defined as having a weight higher than the mean weight of control mice plus one SD. (C) Changes in body weight with age of males from control and the F4 generation progeny of BPA-exposed females (CTL $n = 17$, BPA $n = 26$). (D) Differences in visceral fat and adipocyte size in BPA-F4 versus control males; bar represents 50 μm . (E) Fraction of visceral adipose white tissue with respect to body weight in males from control and BPA-F4 (CTL $n = 12$, BPA $n = 10$). (F) Circulating leptin levels in serum of male mice of different ages from control and BPA-F4 (3 wk old; CTL $n = 7$, BPA $n = 4$, 6 wk old; CTL $n = 8$, BPA $n = 8$, 12 wk old; CTL $n = 8$, BPA $n = 7$). (G) Effect of different concentrations of BPA on the body weight of males from BPA-F2 (CTL $n = 18$, 50 mg $n = 13$, 5 mg $n = 10$, 500 μg $n = 10$, 50 μg $n = 10$). P values were calculated as indicated in the Statistical Analyses of Metabolic Data section of Methods; **** $P < 0.0001$, *** $P < 0.001$, ** $P < 0.01$, * $P < 0.05$, ns not significant (*SI Appendix, Fig. S1*).

weight in the progeny. The results indicate that BPA at concentrations of 50 $\mu\text{g}/\text{kg}$ body weight/day, which are comparable to those to which humans are normally exposed, cause a similar increase in body weight as higher concentrations (Fig. 1G). The relationship between body weight and amount of BPA follows a biphasic, non-monotonic response, as has been described previously (25, 26).

BPA-Induced Obesity Correlates with Increased Food Consumption. In the experiments described above, obesity was observed in the F2 progeny from crosses between two F1 mice from two parallel different exposures (*SI Appendix, Fig. S1A*). In these experiments, BPA could have affected either of the two parental germlines or both. To determine whether the obese epiphenotype can be inherited through the paternal or maternal germlines, we outcrossed the F1 progeny to control unexposed mice of the opposite sex (*SI Appendix, Fig. S2A*). We then measured the body weight of males from the F2 and F3 generations. We find that the median weight increases in the F2 progeny and raises further in the F3 independent of the parental origin of the exposed germline, suggesting that the obese epiphenotype can be inherited through both the paternal and maternal germlines (Fig. 2A). These observations also suggest that the obese phenotype is not the result of external factors such as the maternal environment, transfer of the maternal microbiome, presence of constituents other than sperm in the seminal fluid, etc. To further confirm this, we performed in vitro fertilization (IVF) using purified oocytes from a BPA-F2 female and sperm isolated from the cauda epididymis of a control non-exposed male. The resulting embryos were then implanted into pseudo pregnant unexposed control females, and the weight of their male and female progeny was measured at 10 wk of age.

As controls, CTL-F2 males were directly crossed with BPA-F2 females and vice versa. The results indicate that the median weight of males and females from the IVF experiment is significantly higher than that of unexposed controls (Fig. 2B), suggesting that the overweight phenotype is indeed due to epigenetic changes in the germline rather than external factors.

To gain insights into the physiological processes underlying the obesity phenotype, we housed mice in metabolic cages and measured food intake and energy use during a 3-d period. BPA-F4 males show an increase in total food consumption with respect to controls (Fig. 2C). This increase is due to additional eating during the fasting light cycles (Fig. 2C). In agreement with this observation, control mice show a lower respiratory exchange ratio during the fasting light cycle than during the active dark cycle in each of the 3 d (Fig. 2E and F), indicative of preferential fat utilization during the day when they are asleep (27). Conversely, BPA-F4 males show similar respiratory exchange ratios during the light and dark cycles indicative of constant carbohydrate preference throughout the 3-d metabolic cage test (Fig. 2E and F). The highly significant Time \times Treatment interaction ($P < 0.0001$) shown by a mixed-effects analysis supports the observation that the differences in the respiratory exchange ratio between groups are dependent on the light cycle. However, the energy expenditure of control and BPA-F4 males is the same (Fig. 2G and H). Similar results were obtained when comparing overweight and lean BPA-F6 mice. BPA-F6 overweight males appear to consume more food (*SI Appendix, Fig. S2B*), with increased consumption during the light cycle (*SI Appendix, Fig. S2C*). BPA-F6 lean males show a lower respiratory exchange ratio during the fasting light cycle than during the active dark cycle (Fig. S2D and E), and they spend

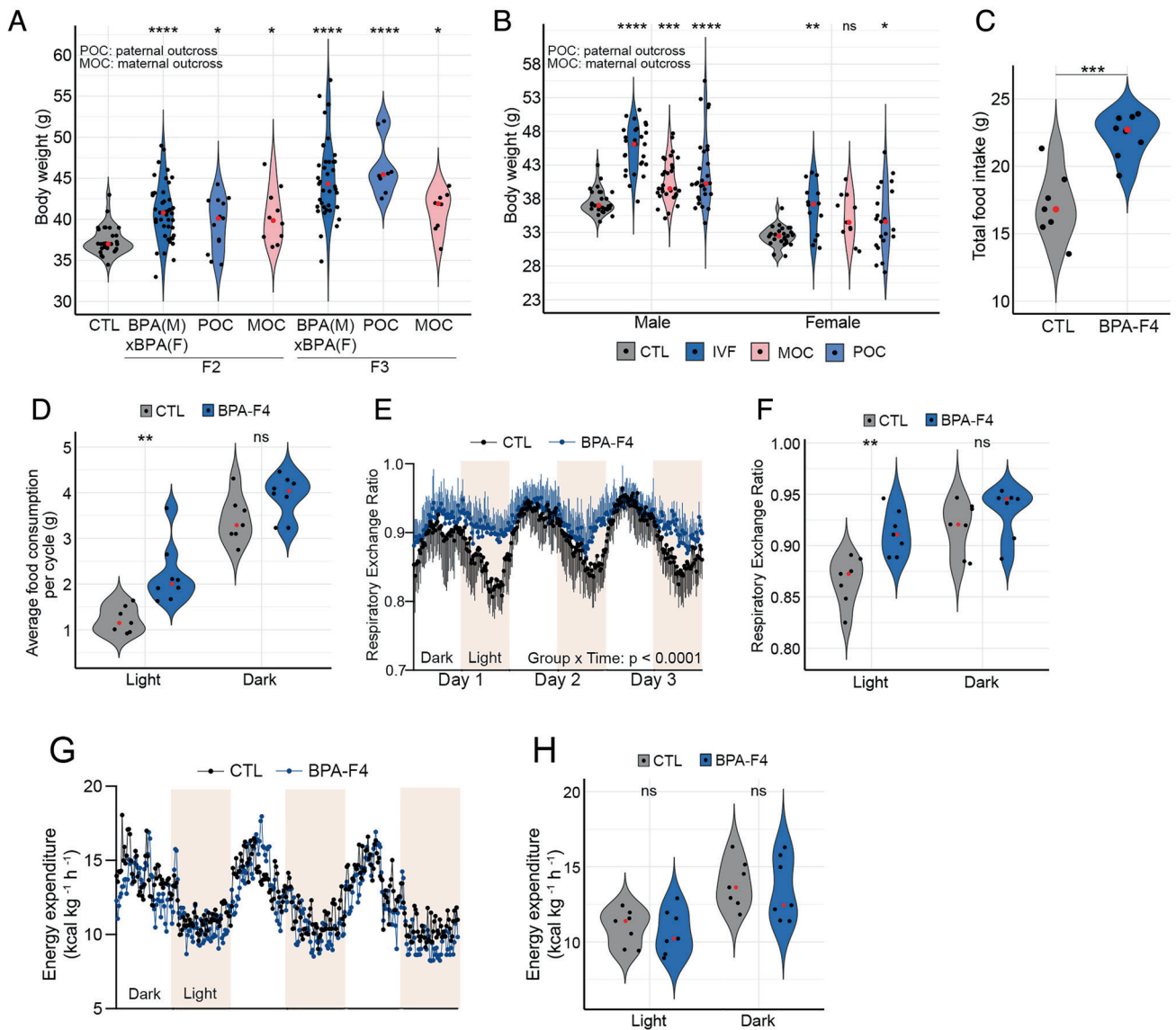


Fig. 2. BPA-induced obesity can be transmitted through the male and female gametes to alter feeding behavior. (A) Differences in body weight in F2 and F3 generation male mice ancestrally exposed to BPA and outcrossed to unexposed controls (CTL). POC, paternal outcross in which a BPA female was crossed to a control unexposed male. MOC, maternal outcross in which a BPA male was crossed to a control unexposed female (CTL $n = 30$ (4 crosses); F2 BPA (M) \times BPA f, $n = 43$ (4 crosses), POC $n = 13$, MOC $n = 10$ (2 crosses each); F3 BPA (M) \times BPA (F) $n = 39$ (4 crosses), POC $n = 8$; MOC $n = 8$ (2 crosses each)). (B) Body weight differences in males and females between control, progeny from IVF experiments, and outcrosses between BPA-F2 and control (Male; CTL $n = 31$, IVF $n = 27$, CTL (M) \times BPA (F) $n = 31$, BPA (M) \times CTL (F) $n = 28$, Female; CTL $n = 27$, IVF $n = 14$, CTL (M) \times BPA (F) $n = 11$, BPA (M) \times CTL (F) $n = 21$). (C) Differences in total daily food intake between control and BPA-F4 males (CTL $n = 7$, BPA $n = 8$). (D) Average food intake by BPA-F4 and CTL males during the light and dark cycles over a 3-d period (CTL $n = 7$, BPA $n = 8$). (E) Respiratory exchange ratio in a 3-d period during the light and dark cycles in control and BPA-F4 males (CTL $n = 7$, BPA $n = 7$). (F) Cumulative respiratory exchange ratio during the light and dark cycles in control and BPA-F4 males (CTL $n = 7$, BPA $n = 7$). (G) Energy expenditure in a 3-d period during the light and dark cycles in control and BPA-F4 males (CTL $n = 7$, BPA $n = 7$). (H) Cumulative energy expenditure during the light and dark cycles in control and BPA-F4 males (CTL $n = 7$, BPA $n = 7$). P values were calculated as indicated in the Statistical Analyses of Metabolic Data section of Methods; **** $p < 0.0001$, *** $p < 0.001$, ** $p < 0.01$, * $p < 0.05$, ns not significant *SI Appendix, Fig. S2*).

the same energy as their overweight siblings (Fig. 2 *F* and *G*). Together, these results suggest that obese mice ancestrally exposed to BPA exhibit unregulated eating patterns that reduce their ability to utilize fat as a fuel source, and expend the same energy as control mice, resulting in increased adiposity.

Activation of CREs in the *Fto* Locus in Sperm Correlates with Transmission of Obesity. Since BPA is an estrogen-like compound that has been shown to act through a variety of nuclear hormone receptors (28), we hypothesized that exposure to BPA may cause alterations in transcription accompanied by a redistribution of TFs throughout the genome of the germline at the time of exposure during E7.5–E13.5, the time of embryonic development

when the DNA of germline cells becomes demethylated. The unmethylated state of the DNA may allow binding of TFs to new sites in the genome where these TFs cannot bind when the DNA is methylated. Subsequently, the presence of bound TFs at these new sites may protect the DNA from re-methylation and these changes may persist in the mature germline as we have previously shown (11). The transgenerational transmission of obesity decreases in the F5 generation, and it disappears in the transition from F6 to F7, suggesting that possible epigenetic alterations induced by exposure to BPA start disappearing in the sperm of F5 and should be absent in F6 sperm. Therefore, to find alterations in TF binding responsible for transgenerational inheritance, we performed ATAC-seq in sperm isolated from the

cauda epididymis of control and BPA F1-F6 males. We used sub-nucleosome-size reads, which correspond to the presence of bound TFs in chromatin (29) and we will refer to sites uncovered by these reads as Transposase Hypersensitive Sites (THSSs).

We first examined the correlation between the transmission of obesity and the presence of altered TF sites in sperm from control and F6 versus F1-F5 mice, which are able to transmit the obese phenotype. We identified 12 sites absent in sperm of control and BPA-F6 but present in BPA-F1-BPA-F5 males, suggesting that all or some of these sites are responsible for the transgenerational transmission of obesity. These 12 sites are present in introns or intergenic regions of various genes and contain motifs for CTCF, AR, ESR1/2, and PPAR γ , suggesting that they correspond to CREs. Examples of five of these sites are shown in Fig. S3 A-D. We then performed *in situ* Hi-C in sperm of control and BPA-F3 mice (30) (see *SI Appendix, Table S1* for a description of quality control steps in the processing of the Hi-C data), we determined statistically significant interactions using Fit-Hi-C (31) and we identified gene promoters with which these differential ATAC-seq sites preferentially interact. The full list of target genes regulated by these putative CREs are listed in *SI Appendix, Table S2*. Many of these genes have been previously shown to be involved in obesity in humans and/or laboratory animals (*SI Appendix, Table S2*). Genes that interact with these putative CREs with the highest frequency are shown in *SI Appendix, Fig. S3F*.

Of the 12 ATAC-seq sites present in sperm of mice ancestrally exposed to BPA and maintained in the F1 to the F5 generations, only one, present in the *Fto* gene, is also present in oocytes after BPA exposure (see below). Therefore, we focused our attention on changes in ATAC-seq located in intron 8 of the *Fto* gene and in a region located distally to *Fto* between the *Irx3* and *Irx5* genes (Fig. 3A). SNPs in the first two introns of the *Fto* gene have been implicated in obesity based on results from genome-wide association studies (GWAS) in humans (32). Site 1 in intron 8 of *Fto* contains binding motifs for the FOXA1 and CTCF proteins (Fig. 3B). ChIP-seq experiments confirm the presence of CTCF at site 1 in the *Fto* gene in BPA-F3 but not in control mice (Fig. 3B, Lower) but we were unable to confirm the binding of FOXA1 to this region using ChIP-seq. Adjacent to this site, several additional ATAC-seq peaks containing motifs for Estrogen Receptor 1 (ESR1), Androgen Receptor (AR), and Peroxisome proliferator-activated receptor gamma (PPAR γ) are either only present in sperm of BPA F1-F5 or their intensity increases in sperm from these animals with respect to BPA-F6 and controls (Sites 2 to 6, Fig. 3B). Sites 2 to 6 were not identified in our original analysis for differential ATAC-seq peaks between BPA-Fi and control because of the stringent statistical conditions imposed in the analysis; however, visual inspection indicates the existence of differential accessibility in a large region of the *Fto* intron containing Sites 1 to 6 (Fig. 3B). These same sites are also accessible in sperm of male progeny obtained from the IVF experiments (Fig. 3B). We will refer to this approximately 4 kb region in intron 8 of the *Fto* gene whose accessibility increases in sperm of the male progeny of BPA-exposed females as the “*Fto* BPA proximal CRE.” In addition, we also observed changes in ATAC-seq signal by visual inspection in a region adjacent to *Fto* located between the *Irx3* and *Irx5* genes (Fig. 3C). This region is not accessible in control mice, but it becomes more accessible in BPA-F1-F5 sperm and loses accessibility in sperm from the F6 generation (Fig. 3C). This region was not identified in our initial analyses of differential chromatin accessibility in sperm of control versus ancestrally exposed mice because the low ATAC-seq signal in the sperm of the F4 generation did not meet the established statistical threshold criteria. The main ATAC-seq peaks in the region contain

motifs for CTCF and AR (Fig. 3C). Thus, this region could represent a regulatory element to which we will refer as the “*Fto* BPA distal CRE.”

BPA-induced TF occupancy at the *Fto* BPA proximal and distal CREs may result in increased interactions with its target genes. To test this possibility and to identify the target promoters of these CREs, we analyzed Hi-C data obtained in sperm of control and BPA-F3 mice using significant interactions identified by Fit-Hi-C (31). The results show a statistically significant increase in interaction frequency in sperm of BPA-F3 mice with respect to control between the *Fto* proximal CRE and other sites in the genome (Fig. 3D). These sites include the *Fto* promoter and several neighboring genes, including *Rpgrip11*, *Irx3*, *Irx5*, *Slc6a2*, and *Mmp2* (Fig. 3E). A similar analysis of the distal CRE indicates that this region shows increased interactions in BPA-F3 sperm relative to control (Fig. 3F) and preferentially interacts with the promoters of *Rpgrip11*, *Fto*, *Irx3*, *Irx5*, and *Mmp2*, as well as the *Fto* proximal CRE (Fig. 3G). The *Rpgrip11*, *Irx3*, *Irx5* genes have been shown to be involved in the regulation of body size and obesity by affecting appetite and food consumption (33–37). These observations therefore agree with findings indicating that BPA-F4 mice display increased food consumption (Fig. 2 C and D). However, the transcript levels for these genes, except for *Mmp2*, are not statistically significantly different between control and BPA sperm (*SI Appendix, Fig. S4A*). Since sperm are transcriptionally inactive, it is possible that the increased interactions between the *Fto* BPA proximal enhancer and target promoters are a vestige of previous transcription during germline development and may have a functional effect after fertilization during pre-implantation development (38).

BPA Induces Changes in Chromatin Accessibility in Oocytes.

Since the obesity epiphenotype elicited by ancestral BPA exposure can also be transmitted through the female germline, alterations in TF binding responsible for obesity should also be present in oocytes. To explore this possibility, we performed ATAC-seq in oocytes from control and BPA-F2 females. Results show that GV oocytes from BPA-F2 females have 478 accessible sites and lack 53 sites with respect to CTL-F2 oocytes (Fig. 4A). Out of the 12 sites present in sperm of BPA-F1-F5 but absent in control and BPA-F6 males, only Site 1 present in intron 8 of the *Fto* gene in sperm of BPA-Fi is also differentially accessible in oocytes (Fig. 4A). This suggests that *Fto* may be the primary effector of transgenerational inheritance of obesity, whereas other differentially accessible sites in the genome may be secondary consequences of *Fto* activation. Sites 2 to 6 present in intron 8 of *Fto* in sperm of BPA-Fi males are not present in oocytes of BPA-F2 females. Instead, different sites in introns 4, 5, and 8 are differentially accessible in oocytes of BPA-F2 females with respect to controls. These sites contain binding motifs for CTCF, FOXA1, TCF21, TBX21, and PPAR γ (Fig. 4A).

CTCF Occupancy at the *Fto* Proximal CRE Correlates with Hypomethylation of DNA in Sperm.

Since binding of CTCF to DNA is known to be sensitive to the methylation status of a specific C located at position 2 in the core motif (39), we obtained base pair resolution GWBS data in sperm from control, BPA-F3, and BPA-F6 mice and examined changes in DNA methylation at the CpG located in this position in the CTCF site present in the proximal CRE. Results show that the level of methylation in this CpG is around 80% in sperm from control males, it decreases to 14% in sperm from BPA-F3 and increases to 50% in BPA-F6 sperm (Fig. 4B). To determine the methylation levels of the CpG present at position 2 in the CTCF motif in Site 1 more quantitatively, we performed bisulfite conversion followed by Sanger sequencing. We find that this C is highly methylated

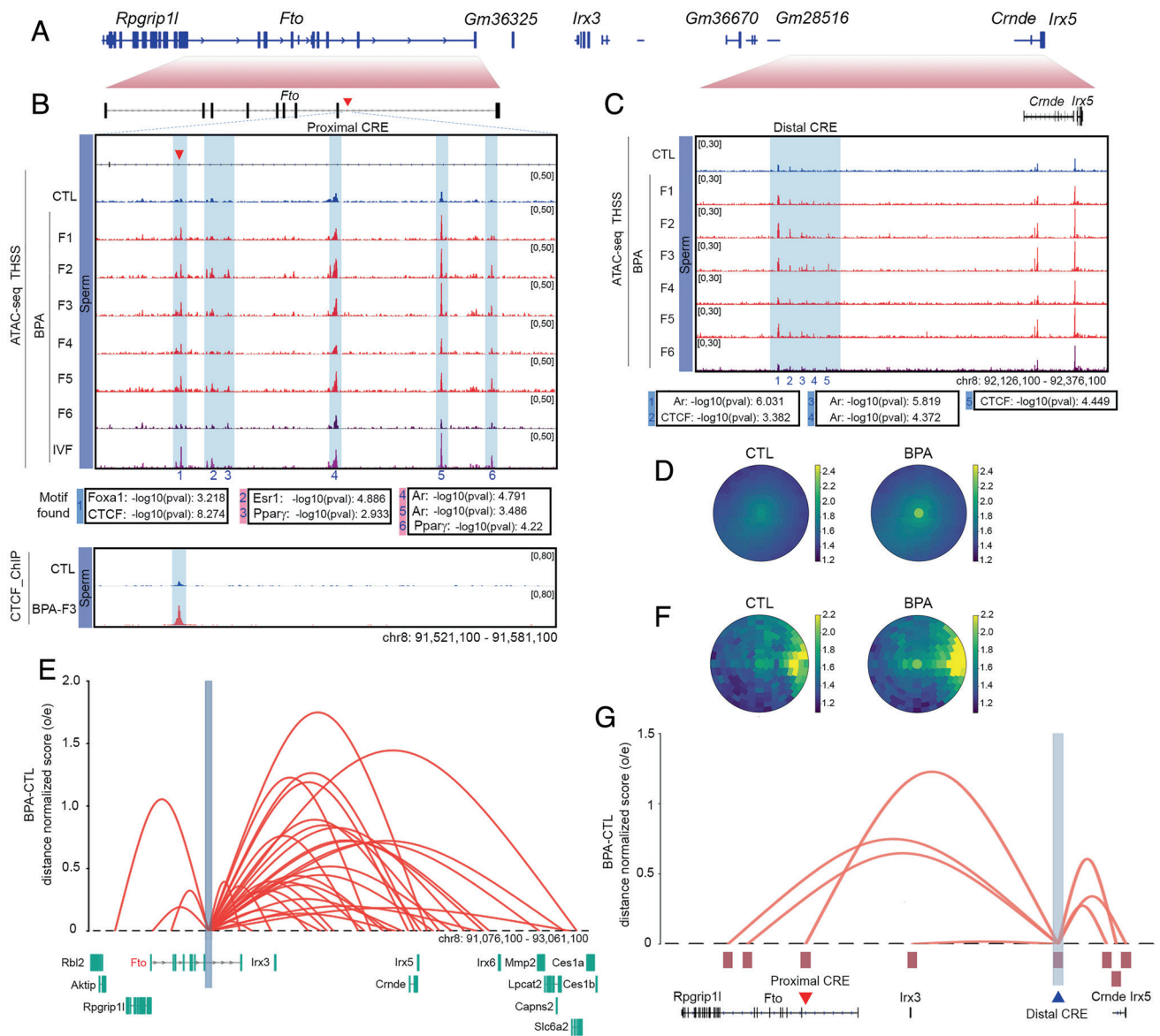


Fig. 3. Changes in accessibility and interactions at two CREs in the *Fto* locus correlate with transmission of obesity. (A) Organization of the region surrounding the *Fto* gene and its relationship to Fig. 3 B and C. (B) Persistence of an ATAC-seq accessible site (Site 1) located in intron 8 of the *Fto* gene in sperm of BPA-F1 through BPA-F5 males. This site contains binding motifs for CTCF and FOXA1, and it is also present in sperm of the male progeny from the IVF experiment. Other sites in the region are present in CTL and BPA-F6 but they increase in ATAC-seq signal in sperm of BPA-F1 through BPA-F5 (Top). ChIP-seq experiments confirm the presence of CTCF at site 1 in sperm of BPA-F3 but not control males (Bottom). (C) Differences in chromatin accessibility at the *Fto* distal CRE between sperm from BPA-F6 and unexposed controls versus BPA F1-F5 males. Differentially accessible sites contain motifs for CTCF and AR. (D) Significant differences in interaction frequency between the *Fto* proximal CRE and other sites in the genome using anchors identified using significant interactions determined by Fit-Hi-C and all Hi-C interactions in sperm of CTL and BPA-F3 mice. The 31 significant Fit-Hi-C interactions between the *Fto* proximal CRE and other sites were analyzed using a bullseye transformed metaplot that depicts distance normalized Hi-C signal in each dataset (P -value = 0.019; unpaired two sample t test). Scores represent average distance-normalized signal. (E) Differential significant Hi-C interactions between the *Fto* proximal CRE and adjacent genomic sites in sperm of BPA-F3 and CTL mice. The Y-axis represents the difference between the distance-normalized Hi-C signal in sperm of BPA-F3 mice and control. (F) Differences in interaction frequency between the *Fto* distal CRE and other sites in the genome using significant interactions determined by Fit-Hi-C and all Hi-C interactions in sperm of CTL and BPA-F3 mice. Ten significant Fit-Hi-C interactions were identified, and the bullseye metaplot score represents average distance-normalized signal in each dataset (P -value = 0.298; unpaired two sample t test). (G) The *Fto* distal CRE preferentially interacts with the *Fto* and *Irx5* genes, including the proximal CRE, in sperm of BPA-F3 versus CTL. The Y-axis represents the difference between the distance-normalized Hi-C signal in sperm of BPA-F3 mice and control (SI Appendix, Fig. S3).

in sperm from control males, is completely demethylated in BPA-F3 sperm, and becomes almost completely remethylated at levels similar to control in BPA-F6 sperm (Fig. 4C). These results agree with the idea that binding of TFs to the unmethylated DNA of the germline at the time of BPA exposure may protect from DNA remethylation to serve as the memory underlying the transgenerational transmission of environmentally induced epiphenotypes. Whether early embryos carry CTCF at this site and whether the ectopic CTCF binding in sperm can be transmitted to early embryos remain to be determined.

Exposure to BPA Results in m⁶A Hypomethylation of an Enhancer RNA in the *Fto* distal CRE. *Fto* encodes a demethylase of N⁶-methyladenosine (m⁶A) in RNA (40). We thus tested whether exposure to BPA affects RNA methylation by measuring m⁶A levels in sperm RNAs of BPA-F3 and control mice. We find a large global decrease in this modification in RNA from sperm of BPA-F3 males with respect to control (Fig. 4D). The absence of m⁶A does not appear to affect stability of sperm RNAs, since global levels of both sense and antisense RNAs are similar in BPA-F3 and control (Fig. 4E). The m⁶A methylation level decreases dramatically between

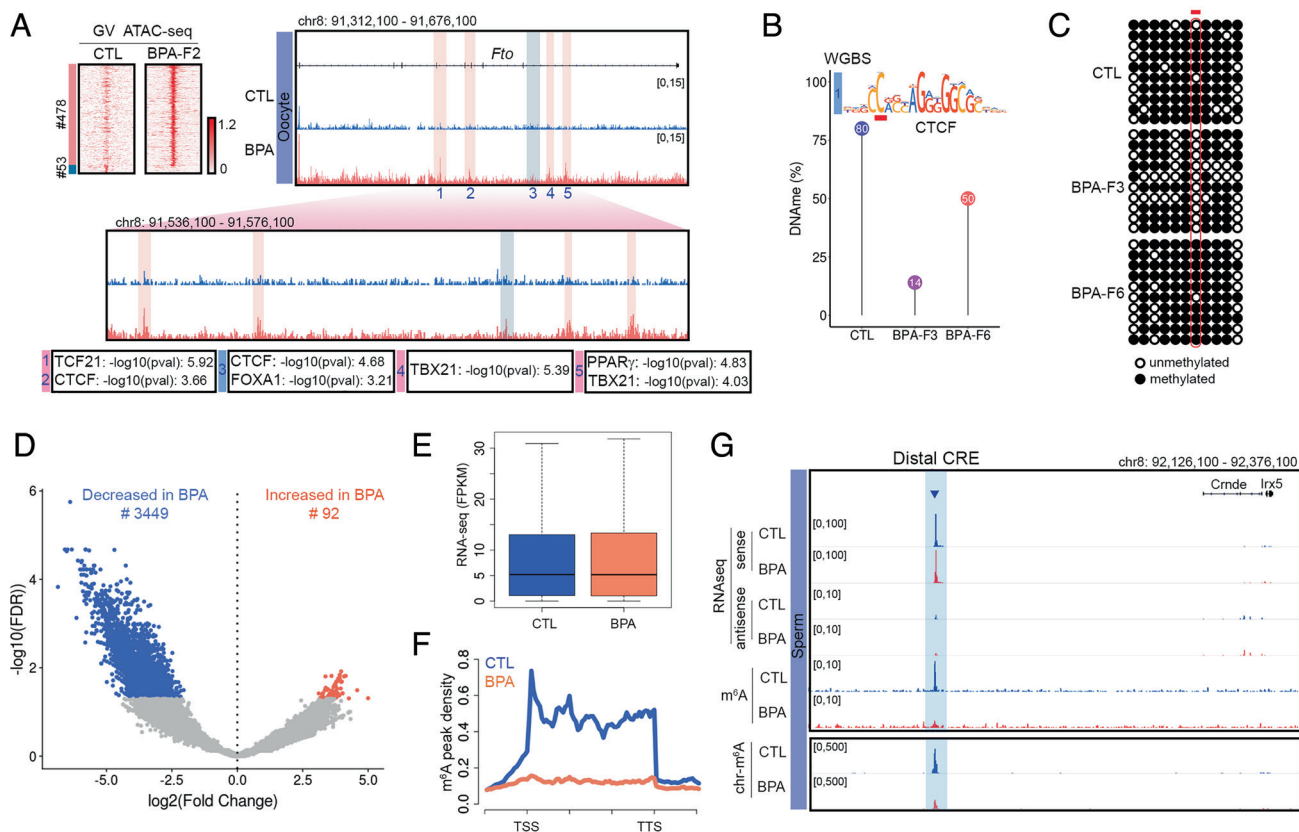


Fig. 4. BPA-induced changes in chromatin accessibility in oocytes, and 5mC DNA and m⁶A RNA methylation in sperm. (A) ATAC-seq sites differentially accessible between oocytes of BPA-F2 and CTL-F2 females. A subset of these sites is located in several introns of *Fto* and Site 3 coincides with Site 1 present in intron 8 in sperm. (B) Methylation levels at the CpG located in position 2 of the CTCF motif present in Site 1 obtained from WGBS-seq in sperm of CTL, BPA-F3, and BPA-F6. (C) Methylation levels at the same CpG obtained from bisulfite sequencing. (D) RNAs whose m⁶A levels are altered in BPA-F3 sperm with respect to control. (E) Global RNA levels are not different between sperm of BPA-F3 and control mice. (F) Levels of m⁶A at sites located in RNAs are lower in sperm from BPA-F3 mice with respect to control. (G) RNA-seq and m⁶A levels in the *Fto* distal CRE. This putative eRNA is present in the fraction of chromatin-associated RNA tightly bound to chromatin (SI Appendix, Fig. S4).

the transcription start site (TSS) and transcription termination site (TTS) of coding and non-coding genes (Fig. 4F). Although some of the m⁶A hypomethylated sites map to mRNAs (SI Appendix, Fig. S4B), most are located in introns and intergenic regions, suggesting that they may be present in enhancer RNAs.

It has been reported recently that m⁶A hypomethylated eRNAs preferentially localize to chromatin where they increase accessibility (41, 42). Analysis of Hi-C data using Fit-Hi-C indicates that putative CRE-encoded eRNAs in which m⁶A levels decrease significantly in sperm of BPA-F3 males with respect to control interact with promoters of genes involved in various processes including development and response to chemicals and organic substances (SI Appendix, Fig. S4C). We thus examined the region surrounding the *Fto* locus for putative eRNAs. We noticed the expression of a ncRNA in the *Fto* distal CRE located between the *Irx3* and *Irx5* genes. Although the levels of this RNA remain the same in control and BPA-F3 sperm, the RNA is m⁶A hypomethylated in BPA-F3 sperm with respect to control (Fig. 4G). To further explore the significance of this putative eRNA, we isolated chromatin-associated RNAs from BPA-F3 and control sperm. We then performed RNA-seq and determined m⁶A levels in chromatin-associated RNAs. Results indicate that the putative eRNA is tightly bound to chromatin and the chromatin-associated fraction is hypomethylated in BPA-F3 sperm with respect to control (Fig. 4G).

Mice Carrying a Deletion of the CTCF Site in the *Fto* Proximal CRE Do Not Become Obese After Ancestral Exposure to BPA. Transmission of BPA-induced obesity correlates with increased

accessibility at sites containing binding motifs for CTCF and several TFs at the *Fto* BPA proximal and distal CREs. To test the involvement of these CREs in the transgenerational transmission of obesity more directly, we used CRISPR to delete a small region surrounding the FOXA1 and CTCF sites in the *Fto* proximal CRE. The binding sites for these two proteins are separated by approximately 90 bp, and although we have direct evidence for the binding of CTCF to this region based on results from ChIP-seq (Fig. 3B), the possible presence of FOXA1 is only inferred from the presence of its motif at the same ATAC-seq peak, which may reflect the presence of CTCF only. We obtained two different mutant strains carrying deletions of 343 bp and 349 bp sequences (SI Appendix, Fig. S5A), which we will refer to as *Fto*^{c1} and *Fto*^{c2}. Neither of these two strains displays any obvious visible phenotypes. After outcrossing, we obtained homozygous strains and examined their response to BPA exposure. The results of these experiments were indistinguishable between the *Fto*^{c1} and *Fto*^{c2} mutant strains and the data presented here as *Fto*^c is the combination of results obtained for each strain separately. *Fto*^c females were exposed to BPA (*Fto*^c_BPA) or vehicle (*Fto*^c_CTL), and F1 progeny from independent exposures were crossed to obtain the F2 generation as described above (SI Appendix, Fig. S1A). Contrary to wild-type (WT) mice, BPA-F2 *Fto*^c mice failed to become obese after ancestral exposure to BPA (SI Appendix, Fig. S5 B and C). F2 *Fto*^c mice were then crossed as described above (SI Appendix, Fig. S1A), and the F3 progeny was analyzed in detail. F3 *Fto*^c_BPA males failed to gain excess weight with age (Fig. 5A), and their weight at 10 wk of age was

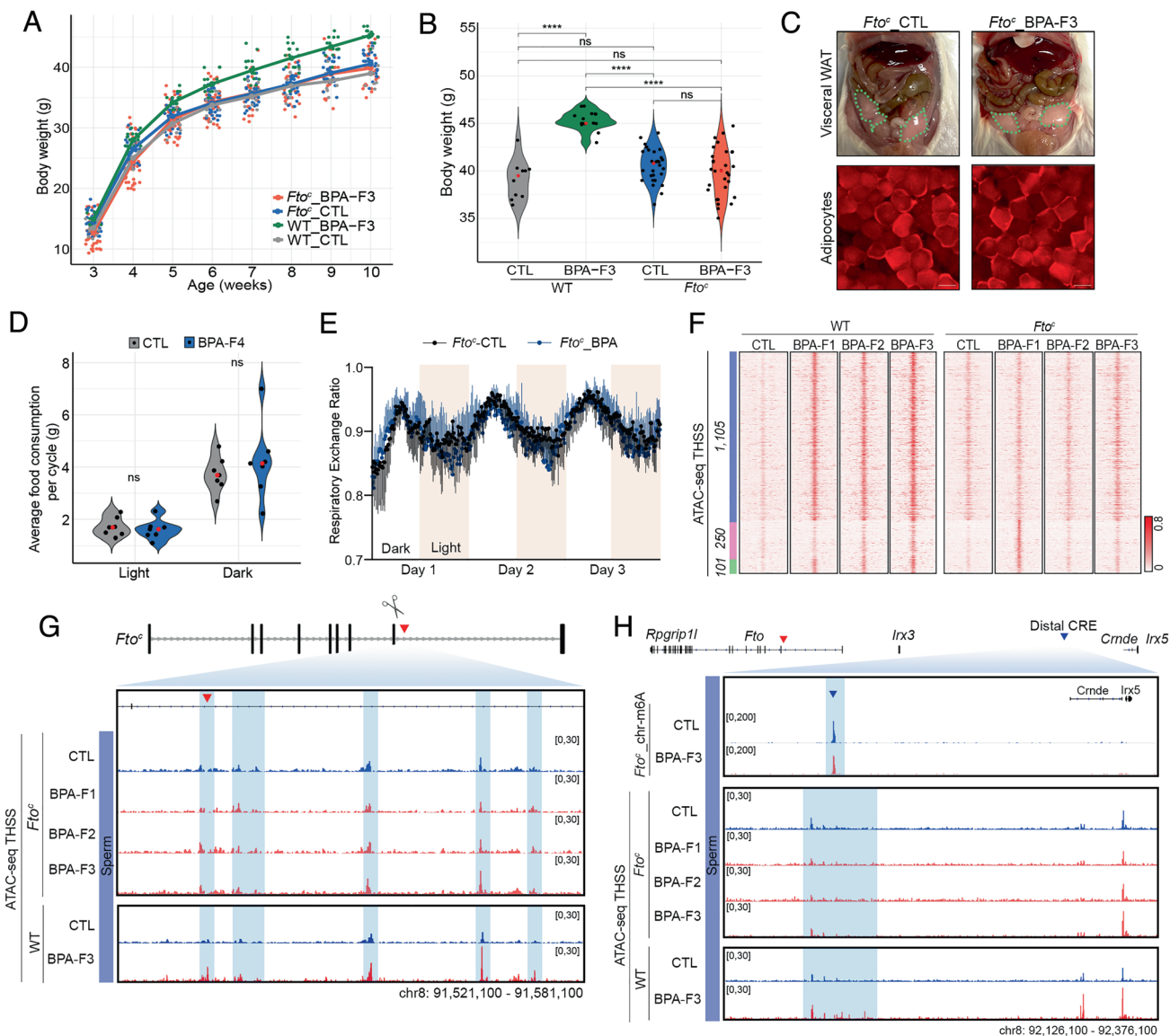


Fig. 5. Deletion of the CTCF site in the *Fto* proximal CRE prevents transgenerational transmission of obesity. (A) F3 *Fto^c* male mice ancestrally exposed to BPA fail to gain weight with age with respect to unexposed *Fto^c*_CTL and WT_CTL (*Fto^c*_CTL *n* = 34, *Fto^c*_BPA *n* = 40, WT_CTL *n* = 15, and WT_BPA *n* = 15). (B) The body weight of 10-wk-old *Fto^c* male mice ancestrally exposed to BPA is the same as that of non-exposed *Fto^c* and WT males but lower than that of exposed WT males (*Fto^c*_CTL *n* = 28, *Fto^c*_BPA *n* = 30, WT_CTL *n* = 10, WT_BPA *n* = 15). (C) 10-wk-old *Fto^c* male mice of the F3 generation ancestrally exposed to BPA do not have excess visceral adipose tissue with respect to unexposed *Fto^c*_CTL (Top). Adipocytes accumulate the same amount of lipids and are the same size in unexposed and exposed *Fto^c* mice (Bottom). (D) *Fto^c* mice ancestrally exposed to BPA at 10 wk of age have the same food intake during the light and dark cycles as unexposed controls (*Fto^c*_CTL *n* = 7, *Fto^c*_BPA *n* = 7). (E) The respiratory exchange ratio, which measures consumption of stored fats versus carbohydrates from a recent meal, is the same in *Fto^c* male mice ancestrally exposed to BPA and unexposed controls (*Fto^c*_CTL *n* = 7, *Fto^c*_BPA *n* = 7). (F) Comparison of chromatin accessibility determined by ATAC-seq in sperm of WT and *Fto^c* male mice unexposed and ancestrally exposed to BPA. Most sites induced by BPA exposure in WT mice do not increase in accessibility in *Fto^c* mice (blue cluster). Only a small subset is induced in *Fto^c* BPA-F1 mice, but they return to normal in the F2 generation (green cluster). Exposure to BPA results in increased accessibility at 250 sites in *Fto^c* but not WT mice, suggesting that deletion of the CTCF site in the proximal enhancer alters the response to BPA. These sites do not persist to the F2 generation (pink cluster). (G) The *Fto* proximal CRE does not show increased chromatin accessibility and TF occupancy in the sperm of *Fto^c* mice ancestrally exposed to BPA compared to unexposed controls. (H) Levels of m⁶A in the eRNA located in the *Fto* distal CRE are not affected in *Fto^c* mice ancestrally exposed to BPA. Chromatin accessibility and TF occupancy in the *Fto* distal CRE is the same in the sperm of *Fto^c* mice ancestrally exposed to BPA compared to controls. *P* values were calculated as indicated in the Statistical Analyses of Metabolic Data section of Methods; *****P* < 0.0001, ****P* < 0.001, ***P* < 0.01, **P* < 0.05, ns not significant (SI Appendix, Fig. S4-5 and S6).

indistinguishable from that of unexposed *Fto^c*_CTL or WT_CTL males but statistically lower than that of WT_BPA mice exposed in parallel at the same time (Fig. 5B). When the weight of 10-wk-old *Fto^c* mice males is compared across generations, no differences among them or with respect to unexposed controls are observed (SI Appendix, Fig. S5D). F3 *Fto^c*_BPA males show the same percentage of visceral fat as controls (Fig. 5C and SI Appendix, Fig. S5E), and the size of the adipocytes is normal (Fig. 5C, Lower). We also examined the SCA-1 positive cells present in the visceral fat tissue of F3 *Fto^c* males by immunostaining with SCA-1

antibodies (SI Appendix, Fig. S5F). The relative number of SCA-1 positive cells, which include adipocyte progenitors but also other cell types, does not increase as a consequence of BPA exposure, and it remains at the same levels in *Fto^c*_BPA and *Fto^c*_CTL as in unexposed WT controls (SI Appendix, Fig. S5G). F3 *Fto^c* males ancestrally exposed to BPA have similar levels of leptin (SI Appendix, Fig. S5H) and food intake as unexposed males (SI Appendix, Fig. S5I), and they consume the same amount of food as controls during the light and dark cycles (Fig. 5D). Furthermore, neither the respiratory exchange ratio (Fig. 5E and

SI Appendix, Fig. S5J) nor energy expenditure (*SI Appendix, Fig. S5 K and L*) is affected by ancestral BPA exposure of *Fto^c* mice. Therefore, deletion of the CTCF site in the *Fto* proximal CRE results in the reversion of all aspects of the obesity epiphenotype induced by exposure to BPA.

The absence of a metabolic response to BPA exposure in mice carrying the *Fto^c* deletion suggests a critical role for the *Fto* proximal CRE in eliciting obesity and its transgenerational transmission. To gain additional insights into the mechanisms underlying this process, we performed ATAC-seq in two biological replicates of sperm from BPA-exposed and unexposed *Fto^c* males from the F1, F2, and F3 generations. Most sites induced by BPA exposure in the sperm of WT mice are not induced in sperm of *Fto^c* males (Fig. 5F, blue cluster), suggesting that these ATAC-seq peaks are a consequence of the activation of the *Fto* proximal CRE rather than of BPA exposure. Only a small subset of sites induced in WT BPA-F1 sperm are observed in *Fto^c* BPA-F1 sperm, but these sites fail to be transmitted to the next generation and disappear in *Fto^c* BPA-F2 sperm (Fig. 5F, green cluster), suggesting again that these chromatin alterations are not responsible for the obesity phenotype or its transgenerational transmission. Interestingly, the deletion of the CTCF site in *Fto^c* mice results in the induction of 250 ATAC-seq peaks in the *Fto^c* BPA-F1 generation that are not induced in WT animals but fail to persist in *Fto^c* BPA-F2 (Fig. 5F, pink cluster). The ATAC-seq peak containing the FOXA1 and CTCF motifs in the *Fto* proximal enhancer is absent in *Fto^c* mice exposed to BPA (Fig. 5G). Surprisingly, other ATAC-seq peaks in the *Fto* BPA proximal CRE containing motifs for ESR1, AR, and PPAR γ remain the same in *Fto^c*_BPA as in *Fto^c*_CTL and in WT_CTL, suggesting that the CTCF site is required for the full TF occupancy and presumed activation of the proximal CRE (Fig. 5G).

The initial analysis of ATAC-seq sites altered in sperm of WT BPA-F1-F5 mice with respect to control and BPA-F6 lead to the identification of 12 differential sites (*SI Appendix, Fig. S3 A–F*). We focused our attention on differential ATAC-seq sites in *Fto* because oocytes contain this but not the rest of the sites. However, it is possible that the other 11 sites of differential chromatin accessibility are also important in the establishment and/or transmission of the obesity epiphenotype. We therefore examined whether exposure to BPA is able to alter chromatin accessibility at these sites in *Fto^c* mice, as is the case in WT. We find that ATAC-seq signal does not increase at any of these sites in sperm of *Fto^c* BPA-F1-F3 mice (*SI Appendix, Fig. S6 A–E*), suggesting that chromatin alterations at these genes are a secondary consequence of the primary changes taking place in the *Fto* proximal CRE after exposure to BPA.

We also examined the state of the distal CRE in mice carrying the CTCF site deletion in the proximal CRE. We find that this CTCF site is also required for the activation of the distal CRE (Fig. 5H). We isolated chromosome-associated RNAs from sperm of *Fto^c* BPA-F3 males and examined m⁶A methylation. We find that the levels of m⁶A in chromosome-associated RNAs, including the eRNA present in the *Fto* BPA distal CRE, do not change in F3 *Fto^c*_BPA male mice with respect to *Fto^c*_CTL, and accessibility at CTCF and AR motifs detected by ATAC-seq remain the same as in control (Fig. 5H). These results indicate that deletion of sequences containing the CTCF site in the *Fto* proximal CRE not only results in the reversion of BPA-induced obesity epiphenotypes and their transgenerational transmission, but it also causes the reversion of all the molecular alterations associated with the phenotypes, supporting a causal relationship between the recruitment of CTCF to the *Fto* proximal CRE and transgenerational inheritance of BPA-induced obesity.

Discussion

Results from several laboratories indicate a correlation between exposures to environmental factors and a variety of phenotypes that can be transmitted transgenerationally in mammals. These observations suggest that environmental exposures can alter the epigenome of germ cells and that these alterations can be transmitted between generations to elicit phenotypes resulting from dysregulation of the somatic cells of the adult. However, the mechanisms by which environmental exposures can give rise to epigenetic alterations that resist the reprogramming events taking place during germline and pre-implantation development remain largely unexplored. Here we find that exposure to BPA results in changes to the epigenome of the male and female gametes manifested by new binding sites for a variety of TFs.

In utero exposure of pregnant females to BPA results in obesity in the F2 generation as an apparent consequence of unregulated eating and increased food consumption. The penetrance of this epiphenotype increases in the F3 and F4 generations but then decreases in F5 and F6, with F7 generation mice showing the same weight as unexposed controls. Comparison of changes in chromatin accessibility in sperm of control and BPA F1–F6 males and oocytes of F2 females with the transmission of obesity suggests a correlation between changes in chromatin accessibility at a CTCF motif in an intron of the *Fto* gene and the transmission of the obesity epiphenotype. Binding of CTCF in response to BPA exposure correlates with changes in DNA methylation at its binding site, suggesting that protein occupancy and DNA methylation may act in concert to establish the memory of ancestral environmental exposures. In addition to CTCF, sperm of obese mice also show increased accessibility at adjacent sites containing binding motifs for several nuclear hormone receptors. Analysis of Hi-C data indicates that this region interacts more frequently with the promoters of *Fto*, *Irx3*, and *Irx5* in sperm of BPA-F3 males than in controls. This region may thus represent a CRE that is not normally bound by TFs in sperm, but becomes occupied after BPA exposure, and this occupied state is transmitted from one generation to the next. The causal role of this region, and the CTCF site in particular, in the transgenerational transmission of BPA-induced obesity is supported by experiments involving mouse strains in which the CTCF site has been deleted. F2 and F3 generation mice carrying a deletion of the CTCF site in the *Fto* proximal CRE fail to become obese after ancestral exposure to BPA, with a complete reversion of every aspect of the behavioral and molecular phenotypes induced by BPA. These observations suggest that the exposed F1 germline is unable to transmit epigenetic alterations induced by BPA when the CTCF site is deleted. The mechanism by which BPA induces binding of CTCF to the *Fto* CRE is unclear. It is possible that BPA binds to nuclear hormone receptors in PGCs and induces their binding to chromatin when DNA is demethylated at the time of the exposure. The presence of proteins bound to chromatin may then interfere with DNA remethylation during germline development after E13.5. CTCF and other TFs present in the mature gametes may remain bound to chromatin after fertilization and again protect the DNA from remethylation in the epiblast. The possibility of transmission of new patterns of TF occupancy between generations is supported by previous findings showing that a subset of chromatin accessible sites in the sperm genome found by ATAC-seq is also present in mouse embryos during preimplantation development (38). Therefore, new patterns of TF occupancy in the gametes caused by environmental exposures could persist in the embryo after fertilization. Once their binding sites are unmethylated, TFs may not need to be bound to DNA continuously during the

differentiation of somatic cells in order to maintain a memory state of accessible chromatin.

In addition to the *Fto* proximal CRE, exposure to BPA also induces increased accessibility at sites containing binding motifs for CTCF and nuclear hormone receptors to a putative distal CRE located between the *Irx3* and *Irx5* genes. This distal CRE encodes a chromatin-associated eRNA. The finding that this and other RNAs are m⁶A hypomethylated in sperm of mice ancestrally exposed to BPA offers an alternative or complementary mechanism to explain the transmission of environmentally induced epiphenotypes by covalent modifications of RNAs. For example, it has been previously shown that tRNA fragments made in the epididymis and transported to sperm are involved in intergenerational transmission of metabolic effects caused by paternal protein restriction or high fat diet (7, 8). In addition, miRNAs present in sperm and transferred to the zygote may cause changes in gene expression affecting the differentiation of adult tissues and have been suggested to be responsible for the transmission of behavioral and metabolic changes caused by early-life traumatic stress (9, 10). It is thus possible that activation of the *Fto* proximal CRE by BPA results in lower levels of m⁶A in RNAs that are then transmitted to the embryo and result in changes in gene expression during early embryonic development. In the case of BPA-induced obesity, preferential persistence of a chromatin-associated eRNA from the distal CRE after fertilization may help maintain the active state of this regulatory region and/or its interactions with the *Fto* and *Irx3/5* genes. A positive feedback loop between the two CREs could contribute to the continued activation of these sequences and the genes they regulate until the epiblast stage when the germline differentiates, and the transmission of this active state between generations.

The mechanisms by which activation of the *Fto* proximal and distal CREs in sperm elicit obesity in the adult are unclear, and their understanding will require additional work in the future. GWAS studies of obese humans have found a strong association between obesity and sequence variants present in regulatory regions located in intronic sequences of the *FTO* gene (43, 44). These CREs carrying sequence variants interact with the promoters of *FTO* and *IRX3* (45). *Irx3* and *Irx5* have been shown to be involved in the differentiation of Agouti-related protein/Neuropeptide Y (AgRP/NPY) and Pro-opiomelanocortin (POMC) neurons in the

arcuate nucleus of the mouse hypothalamus (46). These neurons control appetite and, therefore, possible alterations in *Irx3/5* expression by BPA-mediated changes in *Fto* CREs in specific cell types or times of development may explain the increased food intake observed in mice ancestrally exposed to BPA. The finding that both genetic mutations and environmentally induced epigenetic alterations in the *Fto* gene lead to similar phenotypic outcomes suggests that some of the missing genetic variation required to explain some human diseases may be epigenetic in origin.

Materials and Methods

A detailed description of the materials and methods used in the studies described in the manuscript is provided in the *SI Appendix*. This includes a description of the model system used, isolation of sperm and oocytes, IVF, construction of a mouse strain carrying a deletion of the CTCF site in the proximal CRE, measurements of food intake and leptin levels, ATAC-seq, Chromatin Immunoprecipitation-sequencing (ChIP-seq), bisulfite sequencing, RNA-seq and methylated RNA immunoprecipitation sequencing (MeRIP-seq), and in situ Hi-C. Description of data processing and computational analyses of these data are also provided in the same file.

Data, Materials, and Software Availability. ChIP-seq, ATAC-seq, RNA-seq, m⁶A, and Hi-C data are available from NCBI's Gene Expression Omnibus. The accession number for all the datasets reported in this paper is [GSE149309](https://www.ncbi.nlm.nih.gov/geo/query/acc.cgi?acc=GSE149309). Custom scripts were used to separate ATAC-seq reads into subnucleosomal and nucleosome-size ranges. These scripts are available without restrictions upon request.

ACKNOWLEDGMENTS. We would like to thank Dr. Cynthia Vied at the Translational Science Laboratory of Florida State University for help with Illumina sequencing; Drs. Karolina Piotrowska-Nitsche and Christopher Raymond from the Emory Mouse Transgenic and Gene Targeting Core for their assistance with the IVF experiments and the generation of *Fto* strains. This work was supported by US Public Health Service Awards R01 ES027859 and P30ES019776 (V.G.C.); R35 NS111602, R01 HG008935, U01 MH116441 (P.J.) from the NIH. H.-L.V.W. was supported by NIH F32 ES031827, D.R. was supported by NIH F32 ES034241, and B.J.B. was supported by NIH T32 GM008490. The content is solely the responsibility of the authors and does not necessarily represent the official views of the NIH.

Author affiliations: ^aDepartment of Human Genetics, Emory University School of Medicine, Atlanta, GA 30322

1. J. P. Lim, A. Brunet, Bridging the transgenerational gap with epigenetic memory. *Trends Genet.* **29**, 176–186 (2013).
2. L. Daxinger, E. Whitelaw, Understanding transgenerational epigenetic inheritance via the gametes in mammals. *Nat. Rev. Genet.* **13**, 153–162 (2012).
3. O. J. Rando, Intergenerational transfer of epigenetic information in sperm. *Cold. Spring Harb. Perspect. Med.* **6**, a022988 (2016).
4. L. G. Kahn, C. Philippat, S. F. Nakayama, R. Slama, L. Trasande, Endocrine-disrupting chemicals: implications for human health. *Lancet Diabetes Endocrinol.* **8**, 703–718 (2020).
5. J. A. Hackett, M. A. Surani, Beyond DNA: Programming and inheritance of parental methylomes. *Cell* **153**, 737–739 (2013).
6. O. Rechavi, I. Lev, Principles of transgenerational small RNA inheritance in *Caenorhabditis elegans*. *Curr. Biol.* **27**, R720–R730 (2017).
7. U. Sharma *et al.*, Biogenesis and function of tRNA fragments during sperm maturation and fertilization in mammals. *Science* **351**, 391–396 (2016).
8. Q. Chen *et al.*, Sperm tRNAs contribute to intergenerational inheritance of an acquired metabolic disorder. *Science* **351**, 397–400 (2016).
9. K. Gapp *et al.*, Implication of sperm RNAs in transgenerational inheritance of the effects of early trauma in mice. *Nat. Neurosci.* **17**, 667–669 (2014).
10. A. B. Rodgers, C. P. Morgan, N. A. Leu, T. L. Bale, Transgenerational epigenetic programming via sperm microRNA recapitulates effects of paternal stress. *Proc. Natl. Acad. Sci. U.S.A.* **112**, 13699–13704 (2015).
11. I. Kremisky, V. G. Corces, Protection from DNA re-methylation by transcription factors in primordial germ cells and pre-implantation embryos can explain trans-generational epigenetic inheritance. *Genome Biol.* **21**, 118 (2020).
12. P. J. Murphy, S. F. Wu, C. R. James, C. L. Wike, B. R. Cairns, Placeholder nucleosomes underlie germline-to-embryo DNA methylation reprogramming. *Cell* **172**, 993–1006.e1013 (2018).
13. A. M. Calafat, X. Ye, L. Y. Wong, J. A. Reidy, L. L. Needham, Exposure of the U.S. population to bisphenol A and 4-tertiary-octylphenol: 2003–2004. *Environ. Health Perspect.* **116**, 39–44 (2008).
14. K. Yamasaki, M. Sawaki, M. Takatsuki, Immature rat uterotrophic assay of bisphenol A. *Environ. Health Perspect.* **108**, 1147–1150 (2000).
15. M. Manikkam, C. Guerrero-Bosagna, R. Tracey, M. M. Haque, M. K. Skinner, Transgenerational actions of environmental compounds on reproductive disease and identification of epigenetic biomarkers of ancestral exposures. *PLoS One* **7**, e31901 (2012).
16. M. Manikkam, R. Tracey, C. Guerrero-Bosagna, M. K. Skinner, Plastics derived endocrine disruptors (BPA, DEHP and DBP) induce epigenetic transgenerational inheritance of obesity, reproductive disease and sperm epimutations. *PLoS One* **8**, e55387 (2013).
17. M. Susiarjo *et al.*, Bisphenol A exposure disrupts metabolic health across multiple generations in the mouse. *Endocrinology* **156**, 2049–2058 (2015).
18. F. Xin, L. M. Smith, M. Susiarjo, M. S. Bartolomei, K. J. Jepsen, Endocrine-disrupting chemicals, epigenetics, and skeletal system dysfunction: Exploration of links using bisphenol A as a model system. *Environ. Epigenet.* **4**, dvj002 (2018).
19. R. Klukovich *et al.*, Environmental toxicant induced epigenetic transgenerational inheritance of prostate pathology and stromal-epithelial cell epigenome and transcriptome alterations: Ancestral origins of prostate disease. *Sci. Rep.* **9**, 2209 (2019).
20. I. Sadler-Riggleman *et al.*, Epigenetic transgenerational inheritance of testis pathology and Sertoli cell epimutations: Generational origins of male infertility. *Environ. Epigenet.* **5**, dvz013 (2019).
21. A. Bansal *et al.*, Transgenerational effects of maternal bisphenol: A exposure on offspring metabolic health. *J. Dev. Orig. Health Dis.* **10**, 164–175 (2019).
22. R. Gerona, F. S. Vom Saal, P. A. Hunt, BPA: Have flawed analytical techniques compromised risk assessments? *Lancet Diabetes Endocrinol.* **8**, 11–13 (2020).
23. W. Dekant, W. Volkel, Human exposure to bisphenol A by biomonitoring: Methods, results and assessment of environmental exposures. *Toxicol. Appl. Pharmacol.* **228**, 114–134 (2008).
24. L. N. Vandenberg *et al.*, Urinary, circulating, and tissue biomonitoring studies indicate widespread exposure to bisphenol A. *Environ. Health Perspect.* **118**, 1055–1070 (2010).
25. S. Jenkins, J. Wang, I. Eltoum, R. Desmond, C. A. Lamartiniere, Chronic oral exposure to bisphenol A results in a nonmonotonic dose response in mammary carcinogenesis and metastasis in MMTV-erbB2 mice. *Environ. Health Perspect.* **119**, 1604–1609 (2011).

26. L. N. Vandenberg, Non-monotonic dose responses in studies of endocrine disrupting chemicals: Bisphenol a as a case study. *Dose Response* **12**, 259-276 (2014).
27. D. C. Simonson, R. A. DeFronzo, Indirect calorimetry: Methodological and interpretative problems. *Am. J. Physiol.* **258**, E399-E412 (1990).
28. H. MacKay, A. Abizaid, A plurality of molecular targets: The receptor ecosystem for bisphenol-A (BPA). *Horm Behav.* **101**, 59-67 (2018).
29. J. D. Buenrostro, P. G. Giresi, L. C. Zaba, H. Y. Chang, W. J. Greenleaf, Transposition of native chromatin for fast and sensitive epigenomic profiling of open chromatin, DNA-binding proteins and nucleosome position. *Nat. Methods* **10**, 1213-1218 (2013).
30. Y. H. Jung *et al.*, Chromatin states in mouse sperm correlate with embryonic and adult regulatory landscapes. *Cell Rep.* **18**, 1366-1382 (2017).
31. F. Ay, T. L. Bailey, W. S. Noble, Statistical confidence estimation for Hi-C data reveals regulatory chromatin contacts. *Genome Res.* **24**, 999-1011 (2014).
32. R. J. Loos, G. S. Yeo, The bigger picture of FTO: The first GWAS-identified obesity gene. *Nat. Rev. Endocrinol.* **10**, 51-61 (2014).
33. J. F. M. Carli, C. A. LeDuc, Y. Zhang, G. Stratigopoulos, R. L. Leibel, The role of Rpgrip11, a component of the primary cilium, in adipocyte development and function. *FASEB J.* **32**, 3946-3956 (2018).
34. J. I. Bjune *et al.*, The homeobox factor *Irx3* maintains adipogenic identity. *Metabolism* **103**, 154014 (2020).
35. J. I. Bjune *et al.*, *IRX5* regulates adipocyte amyloid precursor protein and mitochondrial respiration in obesity. *Int. J. Obes. (Lond)* **43**, 2151-2162 (2019).
36. R. Mazar *et al.*, Cleavage of the leptin receptor by matrix metalloproteinase-2 promotes leptin resistance and obesity in mice. *Sci. Transl. Med.* **10**, eaah6324 (2018).
37. R. M. Pirzalska *et al.*, Sympathetic neuron-associated macrophages contribute to obesity by importing and metabolizing norepinephrine. *Nat. Med.* **23**, 1309-1318 (2017).
38. Y. H. Jung *et al.*, Maintenance of CTCF- and transcription factor-mediated interactions from the gametes to the early mouse embryo. *Mol. Cell* **75**, 154-171.e155 (2019).
39. H. Hashimoto *et al.*, Structural basis for the versatile and methylation-dependent binding of CTCF to DNA. *Mol. Cell* **66**, 711-720.e713 (2017).
40. G. Jia *et al.*, N6-methyladenosine in nuclear RNA is a major substrate of the obesity-associated FTO. *Nat. Chem. Biol.* **7**, 885-887 (2011).
41. S. Deng *et al.*, RNA m(6A) regulates transcription via DNA demethylation and chromatin accessibility. *Nat. Genet.* **54**, 1427-1437 (2022).
42. J. Liu *et al.*, N(6)-methyladenosine of chromosome-associated regulatory RNA regulates chromatin state and transcription. *Science* **367**, 580-586 (2020).
43. J. E. Cecil, R. Tavendale, P. Watt, M. M. Hetherington, C. N. Palmer, An obesity-associated FTO gene variant and increased energy intake in children. *N. Engl. J. Med.* **359**, 2558-2566 (2008).
44. M. Claussnitzer *et al.*, FTO obesity variant circuitry and adipocyte browning in humans. *N. Engl. J. Med.* **373**, 895-907 (2015).
45. S. Smemo *et al.*, Obesity-associated variants within FTO form long-range functional connections with *IRX3*. *Nature* **507**, 371-375 (2014).
46. J. E. Son *et al.*, *Irx3* and *Irx5* in *Ins2-Cre(+)* cells regulate hypothalamic postnatal neurogenesis and leptin response. *Nat. Metab.* **3**, 701-713 (2021).